This is an *Accepted Manuscript*, which has been through the Royal Society of Chemistry peer review process and has been accepted for publication.

Accepted Manuscripts are published online shortly after acceptance, before technical editing, formatting and proof reading. Using this free service, authors can make their results available to the community, in citable form, before we publish the edited article. We will replace this *Accepted Manuscript* with the edited and formatted *Advance Article* as soon as it is available.

You can find more information about *Accepted Manuscripts* in the **Information for Authors**.

Chemical Communications

Organometallic chemistry meets crystal engineering to give responsive crystalline materials

A. Bacchi,[a] P. Pelagatti[a]

Dynamically porous crystalline materials have been obtained by engineering organometallic molecules. This feature article deals with organometallic wheel-and-axle compounds, molecules with two relatively bulky groups (wheels) connected by a linear spacer. The wheels are represented by half-sandwich Ru(II) moieties, while the spacer can be covalent or supramolecular in character. Covalent spacers are obtained using divergent bidentate ligands connecting two [(arene)RuX$_2$] groups. Supramolecular spacers are instead obtained exploiting the dimerization of COOH or C(O)NH$_2$ groups appended to N-based ligands. A careful choice of ligand functional groups and X ligands leads to the isolation of crystalline materials with remarkable host-guest properties, evidenced by the possibility of reversibly capture/release volatile guests through heterogenous solid-gas reactions. Structural correlations between the crystalline arrangement of the apohost and the host-guest compounds allows to envisage the structural path followed by the system during the exchange processes.

Introduction

Organometallic chemistry is a discipline which lies at the interface between organic and inorganic chemistry, dealing with compounds which contain at least one M-C bond. The chemical features of the organometallic compounds stem from the perturbation of the stereo-electronic properties the organic ligands experience once bound to the metal. This, and the possibility of combining a number of different metals with a number of different organic C-based donors lead to the construction of M-C bonds characterized by different polarity, robustness and then reactivity. These features have brought organometallic chemistry to be an essential tool for catalysed organic syntheses.[1] More recently, organometallic crystal engineering has attracted interest. The aim of crystal engineering is the fabrication of molecular crystals with desired properties by combining properly functionalized constituent molecules. Since in an organometallic molecule the metal is surrounded, or in some cases even almost completely masked by one or more organic ligands, one could expect that the intermolecular contacts which define its crystal packing are dictated solely by the supramolecular synthons deriving from the interactions of the organic functions present on the ligands. However, this is not always true since the metal often leads to conformational changes and/or to the

modifications of the acid/base character of the organic ligands, with substantial impact on the final intermolecular aggregation pattern. Moreover, the metal itself, when coordinatively unsaturated, can be involved in supramolecular contacts, like in the case of agostic interactions. In a 1996 Chemical Communications feature article[2] Braga and Grepioni anticipated that organometallic crystal engineering could be considered a new discipline, and the topic was comprehensively reviewed by the same authors at the end of 90's.[3] In those works the great potential of organometallic crystal engineering to find out new functional materials was clearly addressed. The growing interest for this topic was subsequently testified by other reviews on the potential role of metal-mediated hydrogen-bonding in crystal engineering, which appeared in 1999, by Brammer,[4] and in the 2000's by Desiraju,[5] Braga and Grepioni.[6] In the same years several papers, clearly titled organometallic crystal engineering, appeared[7]. At that time our ongoing research program was focused on the dynamic behaviour of coordination complexes featuring wheel-and-axle morphology (WAA) towards the reversible adsorption of volatile guests. Differently from rotaxanes,[8] the WAAs of our interest derived from the combination of a linear axle connecting two bulky end groups (Figure 1, top).

The irregular morphology deriving from the dumbbell shape of these molecules frustrates a close packing in the solid state, thus generating soft crystalline frameworks able to reversibly capture volatile guests upon exogenous stimulation.[9] Prior to our work, the literature reported only examples of purely organic WAAs, with some notable examples where the central

a. *Dipartimento di Chimica, Università degli Studi di Parma, Parco Area delle Scienze 17/A, 43124 Parma, Italy, alessia.bacchi@unipr.it.*

axle was a supramolecular cycle deriving from the dimerization of COOH[10] or C(O)NH$_2$[11] groups.
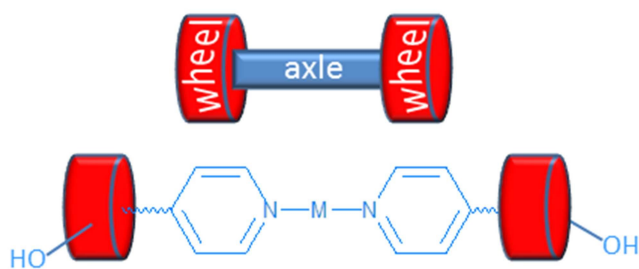

Figure 1 Schematic representation of WAA shaped systems (top); "inorganic" version of WAAD with the metal inserted into the central axle (bottom).

Other literature reported systems dealt with the decoration of the wheels with OH groups which led to wheel-and-axle diols (WAAD), whose clathrating properties were detailed by Toda[12] and served as source of inspiration for the construction, in our laboratory, of "inorganic" WAADs. Here a metal was used for the construction of the central axle, as depicted in Figure 1 (bottom). Two mutually trans OH-functionalized py-based ligands served as wheels. The solid state arrangements and the dynamic host-guest chemistry of several WAADs containing different transition metal ions were deeply investigated in our laboratory.[13] Later on, we became interested in verifying the possibility of fabricating WAAs bearing the metal in the wheels. For reaching the target we chose the organometallic building block [(arene)RuX$_2$] just as wheel. The arene ligand is a benzene or substituted benzene, typically p-cymene, η^6-coordinated to the metal, while the X ligands are halide ligands, typically chlorides. The coordination geometry of Ru can be described as a distorted octahedron where the trihapto arene ligand occupies three coordination sites, the other three being occupied by the two X ligands and by an extra monodentate ligand. At that time (arene)Ru complexes were particularly popular as homogeneous catalysts for selective hydrogenation processes[14] and were acquiring popularity as potential anticancer drugs,[15] whereas their use as building blocks for the construction of supramolecular architectures had received much less attention. In some elegant works Severin showed that partial or complete removal of the halogens followed by the introduction of a polydentate ligand could led to the construction of supramolecular organometallic complexes.[16] Taking into account these considerations, our idea was to maintain the (arene)RuX$_2$ fragment intact and completing the metal geometry with a fourth ditopic ligand which, bridging two [(arene)RuX$_2$] moieties, played the role of axle. In this way, covalent WAA metallorganic compounds (WAAMO) could be designed, as depicted in Figure 2a. The conservation of the halogen ligands on the metal meant to have the possibility of building directional intermolecular hydrogen bonds with properly functionalized ligands of the

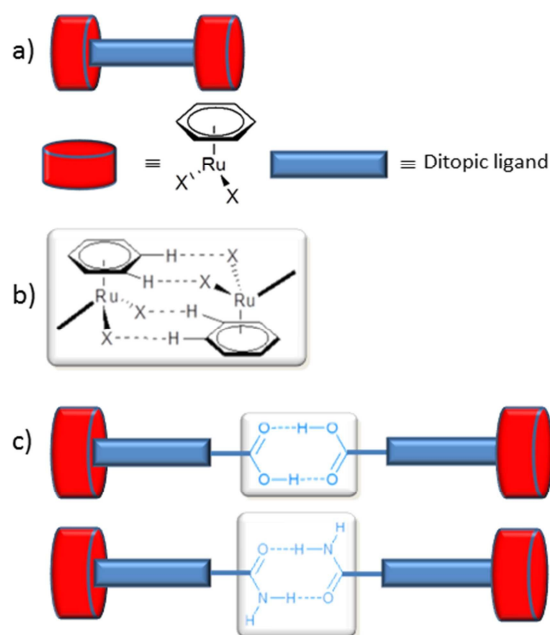type Ru-Cl⋯H-E, where E could be a nitrogen or an oxygen involved in, or close to, the coordination sphere.

Figure 2 Schematic representation of: a) covalent WAAMO; b) inverted piano-stool dimer; c) supramolecular WAAMO based on the dimerization of COOH and C(O)NH$_2$ groups respectively.

Crystal engineered materials based on the hydrogen-bond acceptor character of the halogen ligands had been well described by Brammer[17] and Orpen.[18] Intermolecular contacts involving the second coordination sphere of the metal were thought beneficial for the concatenation of the WAAMO structural units in the solid state, taking into account that the inverted piano-stool dimer depicted in Figure 2b is one of the most recurrent structural motifs found in the solid state chemistry of half-sandwich Ru(II) complexes.[19] Later on, we followed an alternative approach for the construction of the central axle by exploiting robust supramolecular synthon deriving from the supramolecular dimerization of carboxylic or amide groups present on properly chosen ligands. In this way supramolecular WAAMOs could be isolated, as depicted in Figure 2c.

In the case of the amide-based dimers, the N-H bond not involved in the cycle could be exploited as receptor site for hydrogen bond acceptor guests.

These are notable examples of crystal engineered compounds where organometallic building blocks are connected *via* supramolecular interactions, leading to materials based on tailored-shaped supramolecules.

In this feature article we examine the fabrication and the dynamic behaviour towards volatile organic compounds of a large family of crystalline covalent and supramolecular WAAMOs synthesised in our laboratory. The article will be organized into two parts. In Part-I emphasis will be given on

the structural aspects which must be carefully taken into account in order to meet the criteria for the construction of WAAMOs, such as: *i*) nature of the halogen ligands, *ii*) presence of hydrogen-bonding active substituents on the axle, *iii*) solvents used for their syntheses. In Part-II the attention will be moved on the ability of the isolated crystalline materials to reversibly absorb volatile organic compounds through heterogeneous solid/gas reactions. Emphasis will be given to the structural aspects which lead to reversible host/host-guest transformations occurring with complete retention of crystallinity. Some of these are common to Part-I, such as points *i*) and *ii*), while others are specific for triggering reactivity on, such as *iv*) nature of the arene ligand and *v*) length of the organic spacer.

Part-I. Structural features for the WAAMOs assembly

(Arene)Ru(II) complexes are rather easy to synthesise and stable under aerobic conditions, features which make them attractive for crystal engineering purposes where the isolation of high quality crystals is necessary. The Ru source is generally a dinuclear halogen-bridged complex, as the one depicted in Figure 3, which can be isolated, if not commercially available, from the reaction between RuCl$_3$ and the corresponding cyclic diene in refluxing alcohol.[20] The dimer can be easily broken by reaction with a monodentate ligand containing a heteroatom donor, with formation of the corresponding half-sandwich complex (Figure 3).
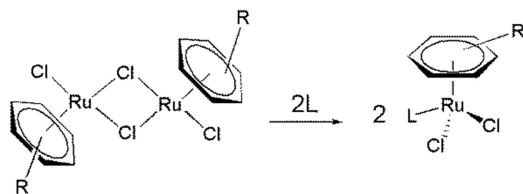

Figure 3 General scheme for the synthesis of (arene)Ru(II) complexes.

Here ruthenium is in a pseudo-octahedral environment, defined by the η^6-coordinated arene, by two chloride ligands and by the divergent ligand L. Depending on the nature of L, covalent or supramolecular WAAMOs can be obtained, as will be shown in the next paragraphs.

Covalent WAAMOs

The construction of covalent WAAMOs was accomplished by using two different classes of covalent divergent organic ligands, *i.e.* pyridine-based and phosphine-based ligands. In all these cases the axles are linear ditopic ligands, where the two donors can be equivalent, like in the case of 4,4′-bipyridyl (**1**),[21] 1,2-di-(4-pyridyl)ethylene (**2**),[21] 1,2-di-(4-pyridyl)ethane (**3**),[21] and 4,4′-bis-(diphenylphosphino)biphenylene (**4**)[22]. In the case of 4-cyanopyridine (**5**)[21] the two donors are different, being a

pyridine and a nitrile one. The ~~ligands~~ chemical structures of the ligands are collected in Figure 4.

All the ligands gave rise to WAA shaped dinuclear complexes where the ditopic ligands bridge two (arene)RuCl$_2$ moieties. Hereafter, the half-sandwich complexes will be denoted by the number indicating the free ligand followed by the Ru symbol, i.e. complexes **1Ru**-**5Ru** are formed by ligands **1**-**5**. The structural characterization of the complexes was possible for **1Ru**, **3Ru**, **4Ru** and **5Ru**, whereas with **2Ru** it was not possible to grow high quality single crystals.
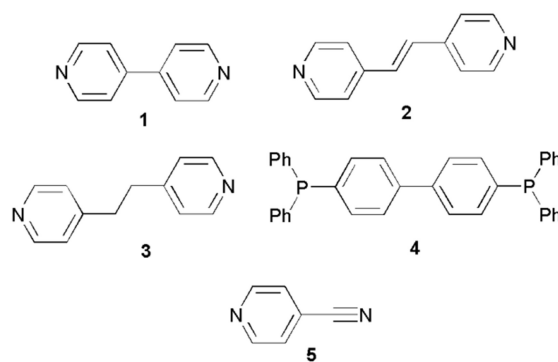

Figure 4 Ditopic ligands used for the synthesis of covalent WAAMOs.

Solubility problems were experienced with complexes **1Ru** and **3Ru**, whose crystals were isolated by free-interface diffusion experiments, starting from solutions of the reagents. Crystals of **4Ru** and **5Ru** were instead isolated by slow evaporation of saturated solutions of the complexes. Importantly, the use of *universal* solvents, such as dmso, was not possible because of the fast ligand solvolysis which led to the formation of the dmso-solvate species [(p-cymene)Ru(κS-dmso)Cl$_2$], as inferred by NMR spectroscopy and X-ray diffraction analysis. The tendency of WAAMOs to generate clathrates were confirmed by several single crystal X-ray analyses. In fact, complex **1Ru** crystallized as MeOH-solvate while complexes **3Ru** and **4Ru** crystallized as dichloromethane-solvates, the last being isolated also as THF-solvate, toluene-solvate and p-xylene solvate. Complexes **2Ru** and **5Ru** were the only examples of not solvate species.

The general structural organization of these compounds is based on the association of the molecules in chains and layers sustained by the ubiquitous supramolecular motif known as the inverted piano stool, Figure 2b, for **1Ru**, **3Ru** and **5Ru**, whereas a layered pattern based on CH…Cl interactions involving phenyls was observed for **4Ru** (Figure 5).

Supramolecular WAAMOs

For the construction of supramolecular WAAMOs the ligands must contain not only a coordinating function but also a group able to generate a robust supramolecular synthon able to create the supramolecular axle by homodimerization.
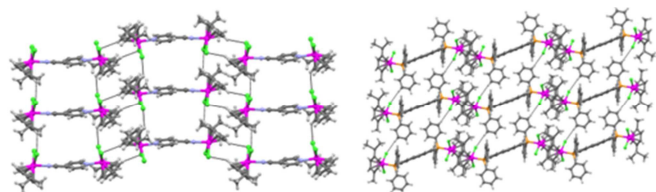
Figure 5 Crystal organization of covalent WAAMOs **5Ru** (left) and **4Ru** (right).

For these reasons we chose pyridines or anilines functionalized with carboxylic or primary amide groups. A chart collecting the chemical structures of the ligands used for the synthesis of the supramolecular WAAMOs is reported in Figure 6. The solid state chemistry of carboxylic acids and amides is characterized by the supramolecular cyclic motifs depicted in Figure 2c, which have been extensively used in crystal engineering,[23] though their reliability diminishes significantly in the presence of competing supramolecular synthons.[24] The first two ligands in Figure 6, isonicotinic acid (**6**) and 4-aminobenzoic acid (**7**), differ in the ability of the coordinating function to create intermolecular hydrogen bond contacts, characteristic which has a profound effect on the final crystal packing arrangement, as will be seen later.
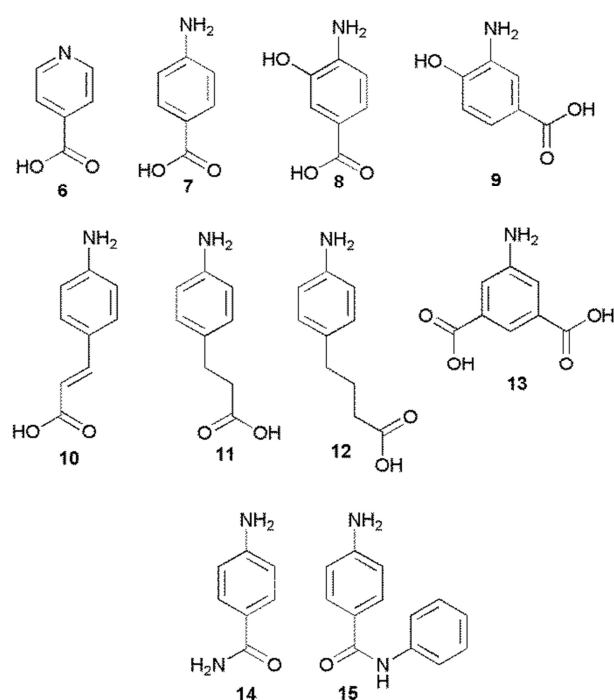

Figure 6 Ligands used for the synthesis of supramolecular WAAMOs.

The introduction of OH groups, like in ligands **8** and **9**, served to verify the possibility of capturing hydrogen bond acceptor guests through intermolecular hydrogen bonds. The effect of the length of the covalent segment of the supramolecular axle was estimated by using ligands **10**-**12**, with the additional

feature that in ligand **10** the spacer is more rigid because of the C-C double bond. The introduction of two carboxylic groups, ligand **13**, allowed to study the possibility of creating more complex supramolecular structures. In the end, the comparison between a primary amide (**14**) and a secondary amide (**15**) made possible to evaluate steric effects on the construction of amide-based WAAMOs. All the corresponding (p-cymene)Ru complexes **6Ru**-**15Ru** were structurally characterized by single crystal X-ray diffraction analysis.

Initially **6Ru** was synthesized and crystallized in dry dichloromethane.[25] The structural analysis revealed the formation of a crystalline phase where the COOH functions preferred to generate intermolecular Ru-Cl…HOOC contacts, thus giving rise to the infinite zig-zag chains depicted in Figure 7, rather than dimerizing. This phase is hereafter referred as **6Ruα**. Indeed, the chloride ligand resulted a better hydrogen bond acceptor than the carbonyl group of the COOH function, a behaviour which confirmed the hydrogen-bond acceptor character of the Cl ligand.[17,18] When **6Ru** was synthesized in not-distilled dichloromethane the hydrate compound **6Ru·H$_2$O** was isolated. The X-ray analysis of the hydrate form showed that two molecules of water bridged two COOH functions of two different organometallic building blocks, thus giving rise to a sort of water-assisted supramolecular WAAMO, whose structure is depicted in Figure 8.
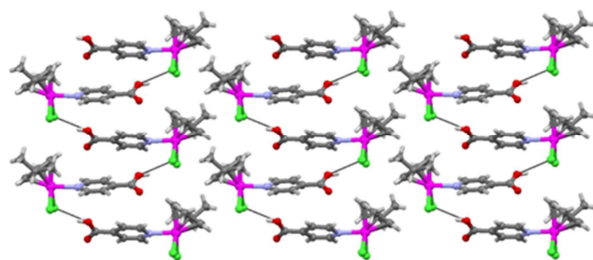

Figure 7 Infinite zig-zag chains sustained by Ru-Cl…HOOC contacts found in **6Ruα**.

Two polymorphs of **6Ruα** were detected, and structurally characterized, on studying the dehydration/hydration process of **6Ru·H$_2$O**.[25,26] In both new polymorphs, **6Ruβ** and **6Ruγ**, the cyclic dimerization of the carboxylic groups was not found and the crystal packings are again based on intermolecular Ru-Cl…HOOC contacts. The structures of **6Ruβ** and **6Ruγ** will be detailed in the next section.

A possible explanation of the missed formation of the supramolecular cycle was found in the mismatch between the number of hydrogen-bond donors (HBD) and the number of hydrogen-bond acceptors (HBA) present in the organometallic building block **6Ru**. In fact, **6Ru** contains three HBAs (one C=O group and two Cl ligands) but only one HBD, the O-H group. This interpretation was tested by synthesizing **7Ru**.[27]

The replacement of pyridine with aniline allowed to balance the number of HBAs (one C=O group and two Cl ligands) with the number of HBDs (two N-H groups and one O-H group).

Indeed, the solid state structure of **7Ru** nicely showed the expected supramolecular dimerization of the COOH functions, with formation of the desired supramolecular wheel-and-axle arrangement (Figure 9).
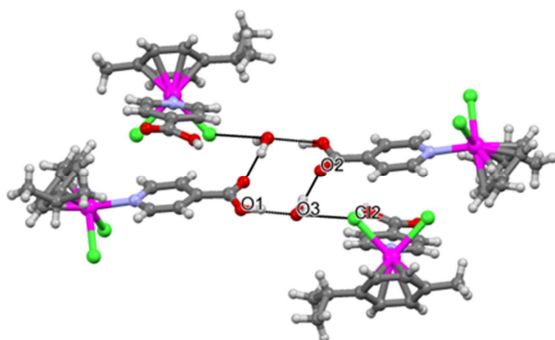

Figure 8 Water assisted supramolecular WAAMO found in **6Ru·H₂O**.

The structural analysis revealed furthermore the key role played by the N-H functions in dictating the final crystalline framework. In fact, each N-H bond contacts a Cl ligand of a neighbouring organometallic building block, thus impeding the involvement of the halogen into intermolecular Ru-Cl…HOOC contacts.
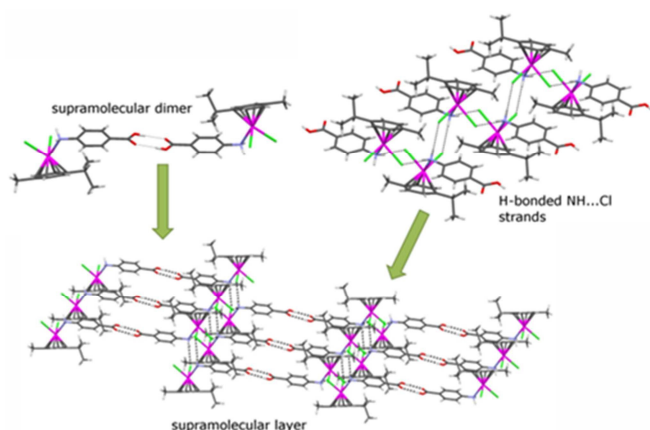

Figure 9 Supramolecular arrangement of complex **7Ru**.

The reaction between **7** and the Ru-precursor in water led again to **7Ru**, highlighting the robustness of the hydrogen bond networks depicted in Figure 9. The supramolecular dimerization of the COOH functions was again found in two polymorphs of the complex [(η⁶-indane)Ru(κN-**7**)Cl₂], where in both cases the N-H groups involved vicinal chloride ligands in intermolecular hydrogen bonds, although in two different arrangements. Reduction of the steric features of the arene ligand led instead to incorporation of water during the crystallization process, as observed in the complex [(η⁶-benzene)Ru(κN-**7**)Cl₂]. The high robustness of the crystalline frameworks containing ligand **7** impeded the formation of host-guest species, both by soaking in and by vapour uptake of

several organic solvents. In order to create more reactive frameworks we tried to augment the cavities present in of the solid network by elongation of the covalent segment of the axle, replacing 4-aminobenzoic acid with 4-aminocynnamic acid (complex **10Ru**).[27] The structural analysis of crystals of **10Ru** grown in acetone revealed the same crystal packing found in **7Ru** but, because of the elongation of the ligand, a molecule of acetone could be hosted into the cavities of the framework (Figure 10).
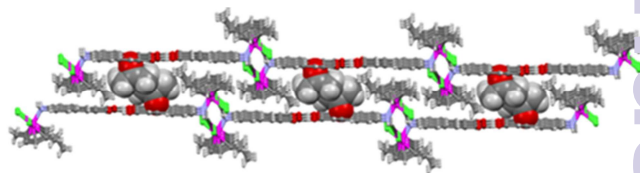

Figure 10 Supramolecular motif found in **10Ru·C₃H₆O** with the molecules of acetone embedded between the layers of the WAAMO units.

The host-guest interactions in **10Ru·C₃H₆O** revealed to be very weak, with degradation of the crystals stored at room temperature because of the loss of acetone. The use of ligands **11** and **12** led to the isolation of complexes **11Ru** and **12Ru**. In these complexes the length of the covalent segment of the axle is similar (**11Ru**) or slightly longer (**12Ru**) than that of complex **10Ru**. However, the absence of the unsaturation makes the alkyl chains more flexible. The X-ray structures of both complexes showed a folding of the C₃ and C₄ chains which led the COOH groups and the N(H)-Ru-Cl system to build a supramolecular association based on O-H…Cl and N-H…O=C hydrogen bonds, thus impeding the formation of the desired supramolecular COOH dimer. In order to reinforce the host-guest interactions without missing the target supramolecular synthons, we moved to the two isomeric ligands **8** and **9**.[29] The introduction of an OH group into the aromatic ring was envisioned as receptor site for HB-active guests, without threaten the two synthons which revealed essential for the construction of WAAMOs, to say the cyclic dimer containing the COOH groups and the N-H…Cl-Ru hydrogen bond networks. The two new crystal engineered chloride complexes **8RuCl** and **9RuCl** crystallized in acetone/chloroform and in neat acetone, without including any molecule of solvent. These structural results were only in partly satisfactorily. In fact, although in both cases the cyclic dimerization of the COOH functions as well as the building of the N-H…Cl-Ru HB contacts were preserved, the absence of acetone into the crystal frameworks was rather discouraging. The analysis of the crystal packings of the two complexes revealed that the OH group was, in both complexes, involved in robust HB-cages (Figure 11, left). Here the hydroxyl group bridges an amino group of a complex and a chloride ligand of a neighbouring molecule.

Attempts to insert acetone, or other volatile organic solvents, into the crystals through heterogeneous solid-gas uptake reactions failed. This partial failure forced us to reconsider

some structural features of the organometallic building blocks. In order to wear, and then render more reactive, the HB-cages found in **8RuCl** and **9RuCl** we decided to replace the chloride ligands with iodide ligands.
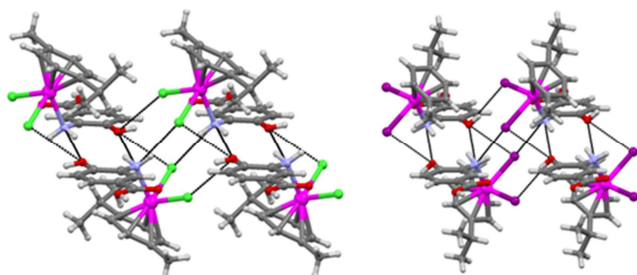

Figure 11 Hydrogen bonded cages sustained by NH and OH groups in **9RuCl** (left) and **9RuI** (right)

The diminishing of HB-acceptor character of the halogen ligand was thought beneficial for triggering the uptake ability of the complexes on. Then, complex **9RuI** was synthesized. Unfortunately, we were not able to isolate complex **8RuI** in a pure form. Complex **9RuI** crystallized in acetonitrile as not solvate. The crystal packing was very similar to the ones found in the chloride complexes, with the molecules associated in supramolecular dimers linked by a HB-network involving all the HB-active groups (Figure 11, right). The only difference was the greater dimension of the HB-cage imposed by the iodine ligand. We were finally delighted to see that complex **9RuI** crystallized as acetone solvate from neat acetone. The crystal structure of **9RuI·C$_3$H$_6$O** showed the preservation of the WAAMO motif with trapping of the guest molecule through HB with the hydroxyl group of the complex, as initially envisaged.[29] Very nicely, complex **9RuI** could be transformed into **9RuI·C$_3$H$_6$O** by heterogeneous uptake of acetone vapours. The process occurred smoothly with complete retention of crystallinity, as demonstrated by XRPD monitoring of the reaction. The details of this solid-to-solid transformation will be discussed in the next section. Apart from aminocarboxylic ligands, we became interested also in the use of aminoamide ligands, such as ligands **14** and **15**. This because the supramolecular synthon based on the cyclic dimerization of amide groups, especially primary amides, is a recurrent structural motif in the solid state chemistry of amides. Two different solvates were isolated with ligand **15**, namely **15Ru·H$_2$O** and **15Ru·C$_2$H$_5$OH**. The included solvent molecules where always hydrogen bonded to the C(O)NHR function, thus hindering the formation of the cyclic dimer.

Differently, complex **14Ru** was crystallized as not solvate in two different polymorphs, hereafter referred as **14Ruα** and **14Ruβ**.[30] As seen with the carboxylic containing systems, here again the NH$_2$ function is involved in intermolecular HBs with chloride ligands. This allowed the amide groups to associate giving rise to the expected cyclic dimers through N-H…O=C hydrogen bonds. The N-H bond not involved in the cyclization contacts a chloride ligand of an adjacent organometallic unit. This self-complementarity of HB functionalities impeded the

insertion of methanol, the solvent of crystallization for both phases, into the crystal lattice. Surprisingly, in **14Ruα** the two dimerizing amide groups are not co-planar, as depicted in Figure 12. This polymorph showed reactivity towards vapour of ammonia, as clearly indicated by the colour change observed for the crystals exposed to gaseous NH$_3$. Unfortunately, the amorphous character and high instability of the final material impeded its characterization.
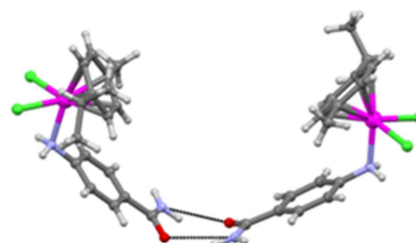

Figure 12 Bent supramolecular dimer in **14Ruα**

This story of the chemical evolution of the supramolecular WAAMO systems towards **9RuI**, capable to uptake and release volatile guests, shows how the tools of modern crystal engineering allow to proceed along an educated trial and error route to achieve a rational design of a crystalline functional material (Figure 13). We can describe this process through three steps of improvement of the chemical structure to achieve the desired functionality: the initial parent molecule **6Ru** was designed to form a supramolecular dimer through the association of the carboxylic acid groups by hydrogen bonds, however the higher strength of the OH…Cl hydrogen bond impeded the formation of the supramolecular WAAMO. We then designed a first generation of modified molecules, by introducing one amino group on the ligand to compete with the OH in bonding to the chlorides and by varying the arene hindrance. Most of the resulting materials had the desired robust supramolecular WAAMO structure, but the packing was not flexible enough to accommodate any guest. Three strategies of mutations of the basic molecule were then attempted in the second generation materials, in order to adapt it to guest uptake: (a) we introduced an OH group on the ligand in different positions; (b) we elongated the ligand; (c) we modified the supramolecular synthon by changing the acid into an amide. These approaches were not completely satisfactory, therefore a third generation of molecules was created, to explore further the molecular variability: systems with longer and more flexible ligands in **11Ru** and **12Ru** were not successful in hosting volatile guests, while the introduction of a substituent on the amide group in **15Ru** allowed guest inclusion but with a different supramolecular pattern. Finally, the modification of the halogen from **9RuCl** to **9RuI** resulted in the successful realization of a material with reversible host-guest properties (Figure 13).

Part II - Dynamic behaviour (solid-gas reactions)

The structural embedding of a gaseous guest into a crystalline phase through heterogeneous solid-gas reactions is of interest in many points of view. In fact, in the case of not solvate starting phases, the so called apohost, such transformations involve the replacing of host-host contacts with new host-guest intermolecular contacts.
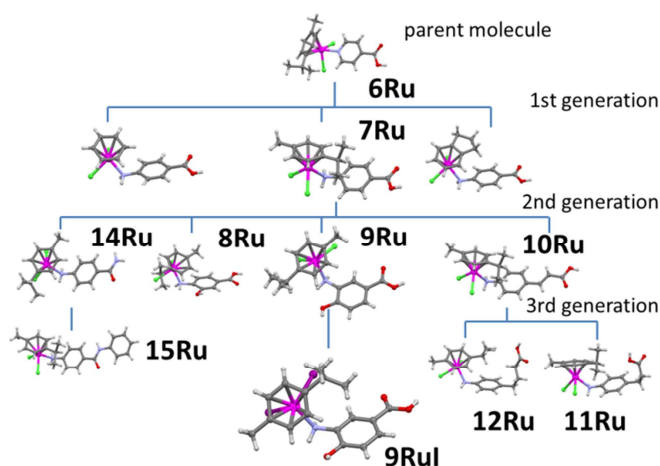

Figure 13 Evolutionary tree from **6Ru** to **9RuI**; refer to Fig. 6 for the legend for the molecular structures.

If the process starts instead from an already solvated material, the guest substitution is favoured if the entering guest is able to give rise to host-guest interactions stronger than the ones present in the initial phase. In both cases then, it is possible to rank the relative intermolecular forces governing the host-host to host-guest transformations. From a practical point of view, these considerations assume a paramount importance in the fabrication of functional materials, such as sensors, heterogeneous catalysts or solids able to trap or separate different volatile compounds with significance, for example, in health and environmental concerns.

The rational design process described in the previous sections and summarized by Figure 13 was aimed at creating the structural conditions needed to generate crystalline molecular materials capable to dynamically adapt their structure in order to accommodate or release small volatile guest molecules. This kind of design was used in the past to formulate the concept of 'venetian blind mechanism' capable to fully rationalize the dynamic porosity of Pd- and Pt- based wheel-and-axle diols.[13] Here we have acted by performing local chemical modifications on the functional groups of our WAAMO host molecules in order to adapt their structures to guest capture and release. We were completely successful in three cases: **4Ru**, **6Ru** and **9RuI**, which showed remarkable reversible host-guest properties by solid-gas processes; for **6Ru** and **9RuI** we were able to figure out a plausible structural path for the process of guest release and uptake. In general, solvation and desolvation processes have been described from a

macroscopic point of view by geometric models of kinetics for interface advance,[31] or from a molecular point of view by investigating the structural implications of the phase transitions.[32] We here embrace this latter view of the phenomena and use structural correlations between the crystalline arrangements of the apohost and the host-guest compounds to envisage the structural path followed by the system during the exchange process. This implies continuous modification of one or few structural parameters that can vary without loss of contact between neighbouring molecules, commonly related to molecular rotations, small displacements, or conformational rearrangements.

Solvation and desolvation processes with covalent WAAMOs

As regards the covalent WAAMOs, solid-gas reactions were clearly observed with complex **4Ru**.[22] **4Ru** was isolated in diethyl ether as not solvate species. The synthesis carried out in THF led instead to the isolation of a solvate species of formula **4Ru·1.5THF**. The removal of the solvent molecules by thermal treatment (120 °C for 13 hours) led to the isolation of the new apohost phase **4Ru'** (Figure 14).
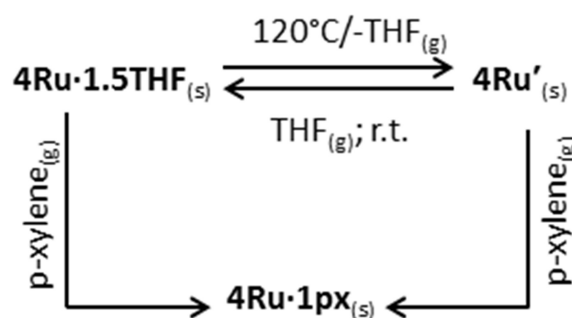

Figure 14 Dynamic transformations observed with complexes **4Ru·1.5THF** and **4Ru'** through heterogeneous solid-gas reactions.

The thermally induced desolvation of **4Ru·1.5THF** provoked a partial loss of crystallinity, as evidenced by the poorly resolved PXRD trace of **4Ru'**. Nicely, exposure of **4Ru'** to vapors of THF at room temperature for 24 hours led to restoration of **4Ru·1.5THF** with full regain of crystallinity, as evidenced by XRPD analysis (Figure 14). Moreover, soaking of **4Ru** in neat THF at room temperature overnight led again to **4Ru·1.5THF**. All these transformations indicate that the wheel-and-axle shape of **4Ru** leads to polymorphs (**4Ru** and **4Ru'**) or pseudo-polymorphs (**4Ru·1.5THF**) featured by dynamic crystalline frameworks able to reversibly rearrange one into each other under exogenous stimuli. Later on, we became interested in verifying if it was possible to exchange THF contained in **4Ru·1.5THF** with aromatic guests, such as benzene, toluene, xylene isomers and p-cymene. These guests were chosen for their health and environmental importance and because their separation is made difficult by the similarity of their boiling points, this last aspect being true especially for the xylene

isomers. In addition, we tested also two acetylenic substrates such as phenylacetylene and 4-ethynyltoluene, which are typical impurities of olefins obtained by naphtha cracking and can act as catalyst poisons in olefins polymerization processes. Exposure of **4Ru·1.5THF** to vapors of the different volatile organic compounds at room temperature for 24 hours, led to a series of new host-guest species, with the general formula **4Ru·xGuest**, where x was dependent on the guest. The uptake processes were monitored by NMR spectroscopy and TGA analysis in order to determine the final host-guest ratio. All the final materials were checked by XRPD analysis in order to verify their crystalline nature. The results indicate that only in the presence of p-xylene THF was quickly (within 5 hours) and quantitatively substituted with formation of the solvate species **4Ru·px**, which considers a host/p-x ratio of 1 to 1. With the other aromatic guests variable amounts of THF were retained in the final materials. Substituted benzenes were more able to exchange THF than benzene, while highly branched guests, such as p-cymene, completely blocked the reaction. The high exchange capability of the substituted benzenes seems to indicate that C-H…π interactions play an important role during the guest exchange process. Although all three xylene isomers were able to remove almost completely THF from the starting material, the amount of p-xylene absorbed was higher than the amount of ox- or m-x absorbed. These results are indicative of the presence of channels in the solid state framework of **4Ru·1.5THF** through which the linear p-xylene can move more easily. However, the lack of structural details for the host-guest species makes hard to reach a complete rationalization of these results. An XRPD monitoring of the THF/p-x uptake exchange revealed a complete retention of crystallinity during the process, with no formation of intermediate amorphous phases, as reported in Figure 15.
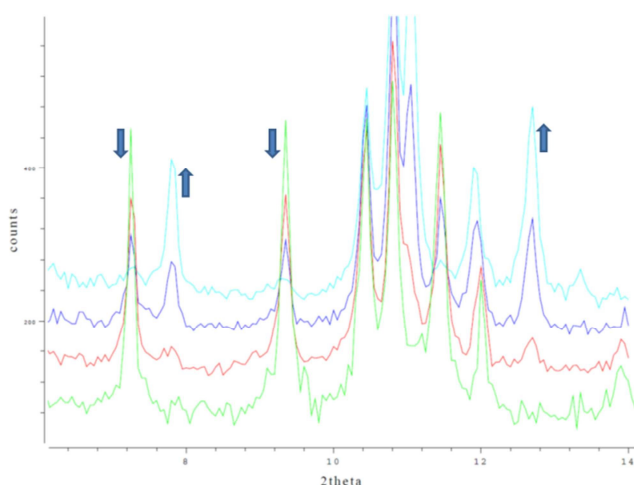

Figure 15 PXRD monitoring of the p-xylene uptake by complex **4Ru·1.5THF**.

The linearity of the two alkyne substrates led again to a complete THF replacement, with formation of two new host guest systems of formula **4Ru·0.3PhC$_2$H** and **4Ru·1.5EtTol**. The phenylacetylene containing product revealed to derive form

partial decomposition of a different phase containing a higher amount of guest formed during the uptake. In fact, an XRPD monitoring of phenylacetylene adsorption showed the formation of a new phase stable only under phenylacetylene vapors, characterized by a high degree of crystallinity. This solid in the absence of guest vapors loses phenylacetylene completely within 24 hours at room temperature, giving rise to a guest free species characterized by an XRPD trace very similar to the one of **4Ru**. **4Ru·1.5EtTol** revealed instead to be completely stable at room temperature, pointing out the importance of C-H…π interactions for the stabilization of the final host-guest species.

Solvation and desolvation processes with supramolecular WAAMOs

Supramolecular wheel-and-axle compounds where the axle is based on the homomeric dimerization of COOH or C(O)NH$_2$ groups were isolated with ligands **7**-**10** and **14** (complexes **7Ru**-**10Ru** and **14Ru**). With the other ligands the construction of the supramolecular dimers was impeded by intermolecular hydrogen bonds involving chloride ligands or molecules of solvent. With the exception of complex **6Ru**, which showed an interesting reactivity towards water, the complexes avoided of the supramolecular dimeric synthon revealed to be inert towards the uptake of gaseous guests. With regard the supramolecular dimeric complexes, the robustness of the hydrogen bond network of **7Ru** based on the contacts developed by the COOH and NH$_2$ groups revealed to prevent solid-gas reactivity. However, the crystal engineered complex **9RuI** was instead reactive towards vapor of acetone. In the following paragraphs the mechanisms governing these solid to solid transformations will be highlighted.

Hydration and dehydration mechanism for 6Ru
The dynamic behaviour of the crystalline networks containing isonicotinic acid was evidenced by the hydration/dehydration process which **6Ruα** can undergo through solid-state reactions. These occurred by a rather complicate mechanism involving three different anhydrous polymorphic forms of **6Ru**. A deep SS NMR (^{1}H DQ CRAMPS)/VT-XRPD/DFT combined study allowed the structural characterization of all the involved polymorphs and, furthermore, confirmed that all the phase-transitions occurred with complete retention of crystallinity. Molecules in **6Ru** are organized in chains of OH…Cl hydrogen bonds (Figure 7 and 16a), with a periodicity of 7.27Å. In **6Ru·H$_2$O** the molecules are similarly organized in chains, whereby the water molecules bridge COOH and Cl groups. The translational periodicity is c=7.42Å and consecutive molecules are rotated by about 90° along the chain direction (Figure 16a-b). During the hydration process of **6Ru**, a water molecule is inserted in the OH…Cl contact, while simultaneously the WAAMO molecules rotate by 45° along the chain (Figure 16c); the rotation brings carboxylic groups of neighbouring chains to face each other (Figure 16d), triggering the formation of the supramolecular WAAMOs previously shown in Figure 8. Interestingly, the dehydration of **6Ru·H$_2$O**

does not proceed by the reverted path, since a competitive anhydrous polymorph exists, **6Ruβ**, that has a structural arrangement very close to the one found for the hydrate complex, with molecules similarly rotated around the hydrogen bonded OH…Cl chains (Figure 17).
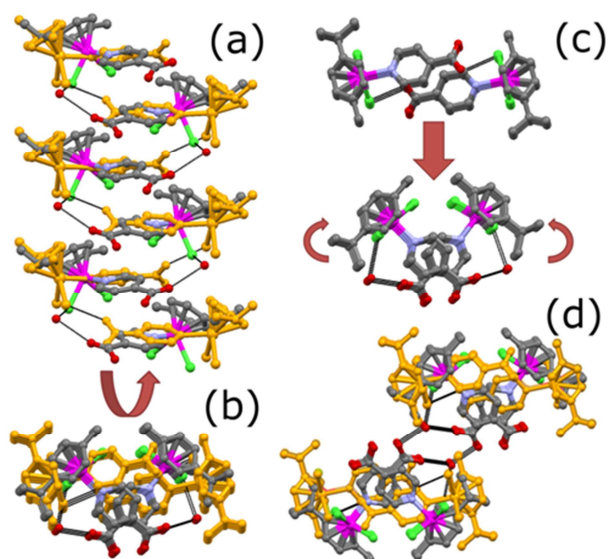

Figure 16 (a) Comparison between chains involving hydrogen bonds (dashed) to chlorine in **6Ruα** (orange) and **6Ru·H$_2$O** (multi-colour), side-view (top) and (b) top view (bottom); (c) suggested rotational mechanism for the conversion of chains between **6Ruα** (top) and **6Ru·H$_2$O** (bottom); (d) insertion of water (red balls) between chains of **6Ruα** (orange) triggering the concerted molecular rotation and the formation of water assisted WAAMOs previously shown in Figure 8.

The **6Ruα** polymorph in fact is never obtained by dehydration of **6Ru·H$_2$O** because the structural rearrangement to regenerate it from the hydrate would be less favourable than the minimal one required for the transition **6Ru·H$_2$O → 6Ruβ**. Most interestingly we have been able to isolate a third anhydrous polymorph **6Ruγ**, that is observed as an intermediate structure during the dehydration process of **6Ru·H$_2$O**. Its structure is very similar to both **6Ru·H$_2$O** and **6Ruβ**, confirming the proposed structural path that allows to remove the water from the crystal (Figure 17).

Guest uptake mechanism for 9RuI

Exposure of **9RuI** to vapors of acetone at room temperature led to a clear color change from light brown to black (Figure 18). The monitoring of the uptake reaction by XRPD analysis indicated a continuous process with smooth conversion of the XRPD trace of the starting complex into the one calculated form the X-ray structure of **9RuI·C$_3$H$_6$O**, with no formation of intermediate amorphous phases. After removal of the acetone atmosphere the XRPD trace belonging to **9RuI** was regained together with the original color. We may track the dynamic structural rearrangements during the conversion from **9RuI** to **9RuI·C$_3$H$_6$O** and back by looking at the similarities and

differences of the initial and final stages of the process. During the transformation from **9RuI** to **9RuI·C$_3$H$_6$O** the [(p-cymene)RuI$_2$] group is turned by about 30° around the Ru-I bond and concomitantly the p-cymene ring rotates around the Ru-(η^6-arene) bond axis (Figure 19).
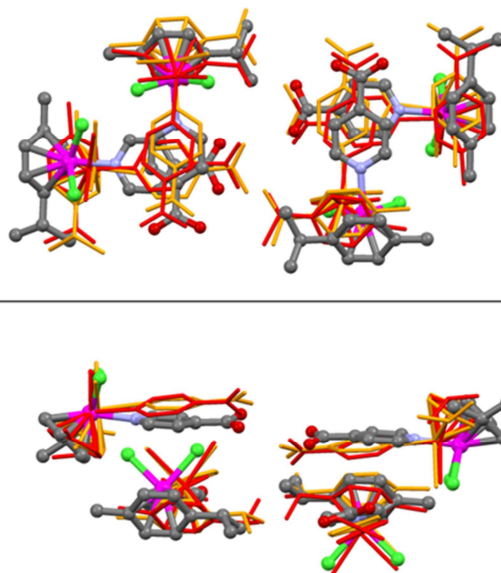

Figure 17 Two perpendicular views of the comparison of the structural arrangements of **6Ru·H$_2$O** (multicolour), **6Ruβ** (red) and **6Ruγ** (orange).

At the same time, the NH…I, NH…OH and OH…I interactions characteristic of the not solvate phase are broken, being replaced by OH…O(acetone) and NH…π interactions in the solvate phase.
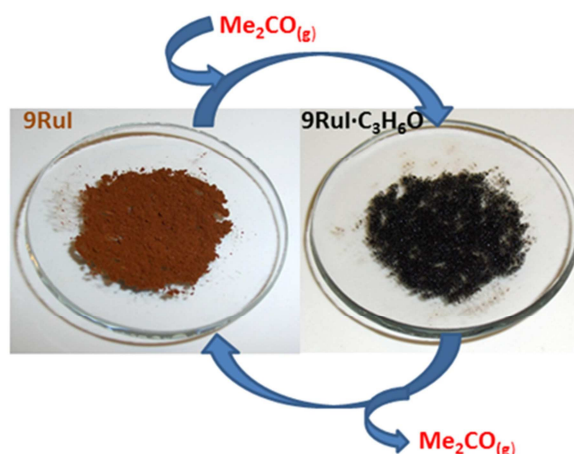

Figure 18 Color change observed during the uptake and extrusion of acetone from **9RuI** and **9RuI·C$_3$H$_6$O**, respectively.

In summary the conversion requires to break and to reform host…host and host…guest hydrogen bonds accompanied by a conformational rearrangement: the OH group that bridges NH and iodine in **9RuI** is displaced, rotates outside and captures

ARTICLE

the incoming acetone by forming one OH…O interaction in **9RuI·C₃H₆O** (Figure 19). This process can be accomplished by local structural adjustments that maintain structural continuity during the process.[33]
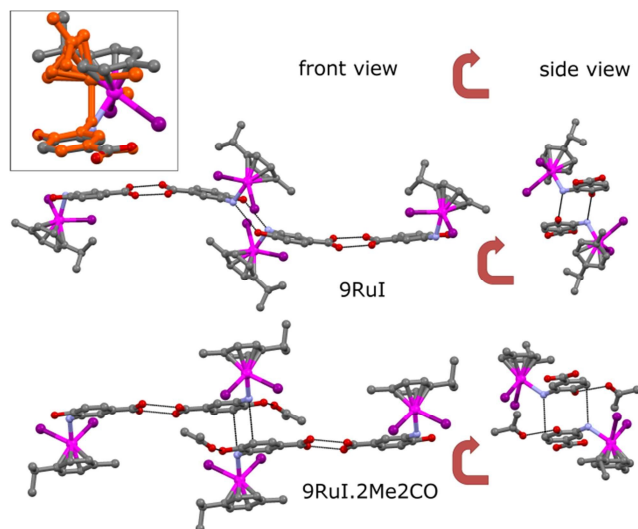

Figure 19 Structural correlations tracking the rearrangement necessary to convert **9RuI** into **[9RuI]₂·2C₃H₆O**. Inset: conformational difference between **9RuI** (orange) and **[9RuI]₂·2C₃H₆O** (color).

Conclusions

In this comprehensive work we have extensively studied the importance of the intermolecular interactions in the crystal packing of the family of WAAMOs based on half-sandwich ruthenium complexes [(arene)Ru(L)Cl₂], a class of molecules that have been extensively studied in bio-organometallic chemistry and homogeneous catalysis. The evolution of these systems towards materials able to reversibly include volatile guests has been pursued by a careful comparison of the effect of small structural local perturbations on the global arrangement, aiming at identifying the most conserved patterns that should logically be based on the most robust interactions. The perturbations concern the arene shape, the length of L, the balance between hydrogen bond donors/acceptors. The molecules have been specifically designed to guarantee a WAA geometry and, in the case of the supramolecular WAAMOs, a perfect match between hydrogen bond donors and acceptors. The covalent WAAMO **4Ru·1.5THF** is characterized by a responsive network, as evidenced by the possibility of releasing and reabsorb THF through solid-to-solid transformations, without loss of crystallinity. Moreover, a selective and complete THF exchange by solid-gas reactions is observed with p-xylene and linear alkynes, while with o-, –m-xylene, benzene and toluene mixed-guest products are

obtained. With regards supramolecular WAAMOs, two robust patterns are usually conserved: the interaction between the NH₂ donor system and the RuCl₂ acceptor system, and the $R_2^2(8)$ cyclic pattern created by the association of the COOH or C(O)NH₂ groups; the latter are far less robust, occurring only in absence of hydrogen bond donors in the crystallization medium. In fact, donating guests are usually inserted between a COOH and a Ru-Cl bond. Also the length and shape of the ligand L may be selected to induce guest inclusion. Based on these considerations, the compounds presented in this work have been designed and tested against guest inclusion. The optimization of all the above factors lead to materials with good performances, where the dynamic properties are based on small reversible structural rearrangements at the local scale, that are amplified to give a controllable collective behaviour. We may regard this optimization as a sort of artificial evolutionary process, where we have tailored mutations in the molecular structures of the complexes, tested the fitness to the expected function, and then selected the best candidates from one generation to the other until the final result has been achieved.

Acknowledgements

Notes and references

[1] D. Steinborn, *Fundamentals of Organometallic Catalysis*, Wiley-VCH, 2012, ISBN: 978-3-527-32716-4.

[2] D. Braga, F. Grepioni, *Chem. Commun.*, 1996, 571.

[3] D. Braga, F. Grepioni, G. R. Desiraju, *Chem. Rev.*, 1998, **98**, 1375; D. Braga, F. Grepioni, *Coord. Chem. Rev.*, 1999, **183**, 19.

[4] J. C. Mareque Rivas, L. Brammer, *Coord. Chem. Rev.*, 1999, **183**, 43.

[5] G. R. Desiraju, *J. Chem. Soc., Dalton Trans.*, 2000, 3745.

[6] D. Braga, L. Maini, M. Polito, E. Tagliavini, F. Grepioni, *Coord. Chem. Rev.* 2003, **246**, 53; D. Braga, F. Grepioni, *Acc. Chem. Res.* 2000, **33**, 601; D. Braga, L. Maini, M. Polito, L. Scaccianoce, G. Cojazzi, F. Grepioni, *Coord. Chem. Rev.*, 2001, **216-217**, 225.

[7] M.-C. Tse, K.-K. Cheung, M. C.-W. Chan, C.-M. Che, *Chem. Commun.*, 1998, 2295; Y. Kim, J. G. Verkade, *Inorg. Chem.*, 2003, **42**, 4262; D. Braga, L. Maini, F. Paganelli, E. Tagliavini, S. Casolari,

Please do not adjust margins **ChemComm**

Journal Name

ARTICLE

F. Grepioni, *J. Organomet. Chem.*, 2001, **637-639**, 609; D. Braga, A. Angeloni, L. Maini, A. W. Götz, F. Grepioni, *New J. Chem.*, 1999, 17; D. Braga, O. Benedi, L. Maini, F. Grepioni, *J. Chem. Soc., Dalton Trans.*, 1999, 2611; S. U. Son, J. A. Reingold, G. B. Carpenter, D. A. Sweigart, *Chem. Commun.*, 2006, 708.

8 M. Xue, Y. Yang, X. Chi, X. Yan, F. Huang, *Chem. Rev.*, doi: 10.1021/cr5005869.

9 D. V. Soldatov, *J. Chem. Crystallogr.*, 2006, **36**, 747.

10 K. R. Jetti Ram, S. S. Kuduva, D. S. Reddy, F. Xue, T. C. W. Mak, A. Nangia, G. R. Desiraju, *Tetrahedron Lett.*, 1998, **39**, 913.

11 C. Malla Reddy, L. Sreenivas Reddy, S. Aitipamula, A. Nangia, C. Lamb, T. C. W. Mak, *CrystEngCom*, 2005, **7**, 44.

12 F. Toda, K. Agaki, *Tetrahedron Lett*., 1968, **33**, 3695.

13 A. Bacchi, E. Bosetti, M. Carcelli, P. Pelagatti, D. Rogolino, *CrystEngCom*, 2004, **6**, 177; A. Bacchi, E. Bosetti, M. Carcelli, P. Pelagatti, D. Rogolino, *Eur. J. Inorg. Chem.*, 2004, 1985; A. Bacchi, E. Bosetti, M. Carcelli, P. Pelagatti, D. Rogolino, G. Pelizzi, *Inorg. Chem.*, 2005, **44**, 431; A. Bacchi, M. Carcelli, P. Pelagatti, *Crystallogr. Rev.*, 2012, 18, 253.

14 R. Noyori, S. Hashiguchi, *Acc. Chem. Res.*, 1997, **30**, 97; M. Yamakawa, H. Ito, R. Noyori, *J. Am. Chem. Soc.*, 2000, **122**, 1466.

15 R. E. Aird, J. Cummings, A. A. Ritchie, M. Muir, R. E. Morris, H. Chen, P. J. Sadler, D. I. Jodrell, *Br. J. Cancer*, 2002, **86**, 1652; F. Wang, A. Habtemariam, E. P. L. van der Geer, R. Fernández, M. Melchart, R. J. Deeth, R. Aird, S. Guichard, F. P. A. Fabbiani, P. Lozano-Casal, I. D. H. Oswald, D. I. Jodrell, S. Parsons, P. J. Sadler, *PNAS*, 2005, **102**, 18269.

16 K. Severin, *Chem. Commun*., 2006, 3859; M.-L. Lehaire, R. Scopelliti, L. Herdeis, K. Polborn, P. Mayer, K. Severin, *Inorg. Chem.*, 2004, **43**, 1609; T. Habereder, M. Warchhold, H. Nöth, K. Severin, *Angew. Chem. Int. Ed.*, 1999, **38**, 3225.

17 L. Brammer, E. A. Bruton, P. Sherwood, *Cryst. Growth Des.*, 2001, **1**, 277; L. Brammer, *Dalton Trans.*, 2003, 3145.

18 G. Aullón, D. Bellamy, L. Brammer, E. A. Bruton, A. Guy Orpen, *Chem. Commun.*, 1998, 653; A. Angeloni, A. Guy Orpen, *Chem. Commun.*, 2001, 343.

19 H. Brunner, M. Weber, M. Zabel, *Coord. Chem. Rev.*, 2003, **242**, 3.

20 M. A. Bennet, T. N. Huang, T. W. Matheson, A. K. Smith, *Inorg. Synth.* 1982, 74.

21 A. Bacchi, G. Cantoni, P. Pelagatti, S. Rizzato, *J. Organomet. Chem.* 2012, **714**, 81.

22 A. Bacchi, S. Bourne, G. Cantoni, S. A. M. Cavallone, S. Mazza, G. Mehlana, P. Pelagatti, L. Righi, *Cryst. Growth Des.* 2015, **15**, 1876.

23 K. R. Jetti, S. S. Kuduva, D. S. Reddy, F. Xue, T. C. W. Mak, A. Nangia, G. R. Desiraju, *Tetrahedron Lett.* 1998, **39**, 913; Z. Quin,

M. C. Jennings, R. J Puddephatt, K. W. Muir, *Inorg. Chem.* 2002, **41**, 5174; S. E. Dann, S. E. Durran, M. R. J. Elsegood, M. B. Smith, P. M. Staniland, S. Talib, S. H. Dale, *J. Organomet. Chem.* 2006, **691**, 4829; T. Beyer, S. L. Price, *J. Phys. Chem. B* 2000, **104**, 2647

24 F. H Allen, W. D. S. Motherwell, P. R. Riathby, R. Snaith, A. E. H. Weatly, *New J. Chem.* 1999, **23**, 25-34.

25 A. Bacchi, G. Cantoni, M. R. Chierotti, A. Girlando, R. Gobetto, G. Lapadula, P. Pelagatti, A. Sironi, M. Zecchini, *CrystEngCom*, 2011, **13**, 4365.

26 M. R. Chierotti, R. Gobetto, C. Nervi, A. Bacchi, P. Pelagatti, Colombo, A. Sironi, *Inorg. Chem.*, 2014, **53**, 139.

27 A. Bacchi, G. Cantoni, M. Granelli, S. Mazza, P. Pelagatti, G. Rispoli, *Cryst. Growth Des.*, 2011, **11**, 5039.

28 A. Bacchi, C. Loffi, P. Pagano, P. Pelagatti, F. Scé, *J. Organomet. Chem.*, 2015, **778**, 1.

29 A. Bacchi, G. Cantoni, F. Mezzadri, P. Pelagatti, *Cryst. Growth Des.*, 2012, **12**, 4240.

30 A. Bacchi, G. Cantoni, D. Crocco, M. Granelli, P. Pagano, P. Pelagatti, *CrystEngCom*, 2014, **16**, 1001.

31 A. L. Galwey, *Termochimica Acta*, 2000, **355**, 181.

32 G. Coquerel, S. Petit, *Chem. Mater.*, 1996, **8**, 2247.

33 T. R. Shattock, K. K. Arora, P. Vishweshwar, M. J. Zaworotko, *Cryst. Growth Des.* 2008, **8**, 4533; J. R. G. Sander, D.-K- Bučar, R. F. Henry, B. N. Giangiorgi, G. G. Z. Zhang, L. R. MacGillivrai, *CrystEngCom* 2013, **15**, 4816.